

## Surface roughness observation by scanning tunneling microscopy using a monolithic parallel spring

H.C. Zhang, A. Sasaki, J. Fukaya, and H. Aoyama

Citation: *J. Vac. Sci. Technol. B* **12**, 1669 (1994); doi: 10.1116/1.587259

View online: <http://dx.doi.org/10.1116/1.587259>

View Table of Contents: <http://avspublications.org/resource/1/JVTBD9/v12/i3>

Published by the AVS: Science & Technology of Materials, Interfaces, and Processing

### Related Articles

Symmetric–asymmetric transformation of an image on GaAs(001)-c(4×4)α surface using scanning tunneling microscopy

*J. Vac. Sci. Technol. A* **30**, 061403 (2012)

Scanning tunneling microscope-based local electroluminescence spectroscopy of p-AlGaAs/i-GaAs/n-AlGaAs double heterostructure

*J. Vac. Sci. Technol. B* **30**, 021802 (2012)

Streamlined inexpensive integration of a growth facility and scanning tunneling microscope for in-situ characterization

*J. Vac. Sci. Technol. B* **29**, 041804 (2011)

Atomic structure and optical properties of InAs submonolayer depositions in GaAs

*J. Vac. Sci. Technol. B* **29**, 04D104 (2011)

Synchrotron photoemission studies on reconstructed strained surfaces

*J. Vac. Sci. Technol. A* **29**, 011003 (2011)

### Additional information on *J. Vac. Sci. Technol. B*

Journal Homepage: <http://avspublications.org/jvstb>

Journal Information: [http://avspublications.org/jvstb/about/about\\_the\\_journal](http://avspublications.org/jvstb/about/about_the_journal)

Top downloads: [http://avspublications.org/jvstb/top\\_20\\_most\\_downloaded](http://avspublications.org/jvstb/top_20_most_downloaded)

Information for Authors: [http://avspublications.org/jvstb/authors/information\\_for\\_contributors](http://avspublications.org/jvstb/authors/information_for_contributors)

### ADVERTISEMENT

**AVS 59<sup>th</sup> International Symposium & Exhibition**  
October 28–November 2, 2012 • Tampa, Florida

**AVS**  
212-248-0200  
avsnyc@avs.org  
www.avs.org



**DIVISION/GROUP PROGRAMS:**

- Advanced Surface Engineering
- Applied Surface Science
- Biomaterial Interfaces
- Electronic Materials & Processing
- Magnetic Interfaces & Nanostructures
- Manufacturing Science & Technology
- MEMS & NEMS
- Nanometer-Scale Science & Technology
- Plasma Science & Technology
- Surface Science
- Thin Film
- Vacuum Technology

**FOCUS TOPICS:**

- Actinides & Rare Earths
- Biofilms & Biofouling: Marine, Medical, Energy
- Biointerphases
- Electron Transport at the Nanoscale
- Energy Frontiers
- Exhibitor Technology Spotlight
- Graphene & Related Materials
- Helium Ion Microscopy
- InSitu Microscopy & Spectroscopy
- Nanomanufacturing
- Oxide Heterostructures-Interface Form & Function
- Scanning Probe Microscopy
- Spectroscopic Ellipsometry
- Transparent Conductors & Printable Electronics
- Tribology

# Surface roughness observation by scanning tunneling microscopy using a monolithic parallel spring

H.-C. Zhang

Changchun Institute of Optics and Fine Mechanics, Changchun, Jilin Province, People's Republic of China

A. Sasaki, J. Fukaya, and H. Aoyama

Faculty of Engineering, Shizuoka University, Johoku, Hamamatsu 432, Japan

(Received 9 August 1993; accepted 16 September 1993)

A new scanning tunneling microscope (STM) and its application to surface roughness observation are described. Precision two-dimensional positioning of our STM instrument was achieved with a two-dimensional parallel spring driven by two stacked piezoelectric actuators (PZT), so that the mutual interference effect between  $x$ - and  $y$ -axis displacements is very small. The PZT for the  $z$ -axis displacement and control was mounted on the monolithic parallel spring. Therefore, the mutual interference effect of three-dimensional displacements is negligible. We have applied this STM to observation of surface roughness. A block gauge and a gold thin film evaporated on glass plates are observed at the constant-current mode and the zero bias voltage.

## I. INTRODUCTION

Scanning tunneling microscopy (STM) has been proven and developed to be a powerful tool in surface science and engineering.<sup>1-3</sup> Using an STM probe, we can obtain not only three-dimensional images of surface roughness but also information on the electronic and mechanical nature of the surface. The STM scanners have been developed with piezoelectric actuators. The scanner types were tripod,<sup>4</sup> single piezoelectric tube,<sup>5</sup> and stacked piezoelectric disks with a mechanical amplifier, which was suitable for scanning large areas (hundreds of microns), but had a low mechanical resonant frequency ( $\leq 150$  Hz).<sup>6-8</sup> The three-dimensional displacements of the tripod type, the cross type, and the piezoelectric tube type have mutual interference in the  $x$ -,  $y$ -, and  $z$ -direction displacements. In the case of the tripod type, the amount of interference is 0.1%–1%.

In this article, we have developed a new STM system with small mutual interaction and relatively high resonant frequency using a monolithic parallel spring having no displacement amplification. We demonstrate that our STM is a useful tool to observe the surface morphology or surface roughness at real time, and properties of block gauges and gold thin films.

## II. DESIGN OF THE STM INSTRUMENT

### A. STM system

Figure 1 shows a schematic diagram of the STM system that was constructed in our laboratory. The tunneling current is converted to a voltage signal using the current-to-voltage ( $I-V$ ) converter, which is constructed with a low offset bias current operational amplifier (3 fA, OPA104AM Burr-Brown). This low value is applicable to observe images at the zero bias voltage, that is, to control using the tunneling current noise, which is generated at the tunneling resistance.<sup>9</sup> In this observation method, the STM system is required to have a low electronic and mechanical noise.<sup>10-12</sup> The tunneling current signal is fed to the controller, which consisted of an amplifier, an absolute amplifier, a log amplifier, an inte-

gral control amplifier, and a high-voltage amplifier, as shown in Fig. 1. The absolute amplifier (AD630 Analog Devices) is a rectifier to operate under the zero bias voltage operation.

### B. STM unit

Figure 2 shows a schematic diagram of the STM unit. An outer frame of this unit was made of hard aluminum, which was constructed with two monolithic mechanical parts to achieve a high stiffness and to serve as well as an electrical shield from outside electric disturbances. The small  $xy$  stage has displacement ranges of 3.4 mm. The  $z$  stage has a stroke of about 2 mm using a one-sixth reducing mechanism of the micrometer-head movement.

Figure 3 shows the  $x$ - and  $y$ -displacement mechanism, which uses the two-dimensional monolithic parallel spring (MPS) ( $44 \times 44 \times 10$  mm<sup>3</sup>, 30 gf, and hole diameter of 14 mm). The MPS has small rotation angle components under the displacement; therefore, the relative value of the  $x$ - and  $y$ -direction mutual interference is calculated to be smaller than 0.02% using a simple mechanical link model. The PZT for the  $z$ -axis displacement and control is mounted on the MPS; therefore, fundamentally the  $z$ -direction interference with the  $x$  and  $y$  direction is considered to be very small. Two-dimensional displacements (within 12  $\mu$ m) of the MPS are carried out with two stacked piezoelectric actuators (PZT

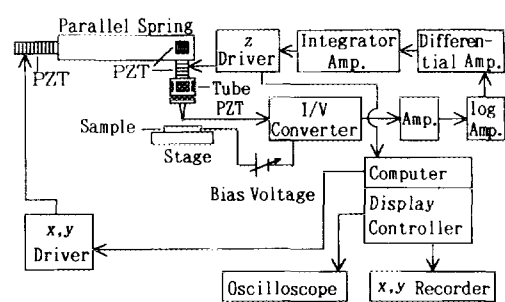


FIG. 1. Schematic diagram of the STM system.

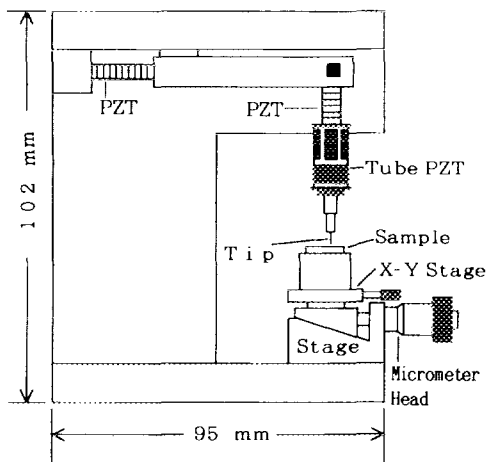


FIG. 2. Schematic diagram of the STM unit.

AE0505D16, NEC Ltd.), and the  $z$ -direction control and displacement (within  $6 \mu\text{m}$ ) with a PZT (NLA5 $\times$ 5 $\times$ 9, Tokin Ltd.). To scan a fine range, the  $x$ -,  $y$ -, and  $z$ -direction displacement are performed using a tube-type piezoelectric transducer (Tokin Ltd.), as shown in Fig. 2.

**C. Dynamic properties of STM unit**

The displacements and dynamic properties of the MPS were measured with an optical fiber displacement sensor. We estimated the spring constant from the relation between load and displacement of the MPS constructed with PZTs. The value of the spring constant was  $0.7 \text{ MN/m}$ , which is nearly the same value of the MPS alone. The frequency response of the MPS was measured using a random noise signal. The sensor signal was input to the fast Fourier transformer, and we estimated the mechanical frequency response and stiffness of the STM displacement mechanism. The experimental results are shown in Figs. 4 and 5. Figure 4 shows the  $z$ -direction mechanical frequency response, which has the high mechanical resonant frequency of  $1.3 \text{ kHz}$ . Figure 5 shows the  $x$ -direction frequency response, which has the resonance frequency of  $1.05 \text{ kHz}$ , and the  $y$ -direction frequency response has the similar value to the  $x$  direction.

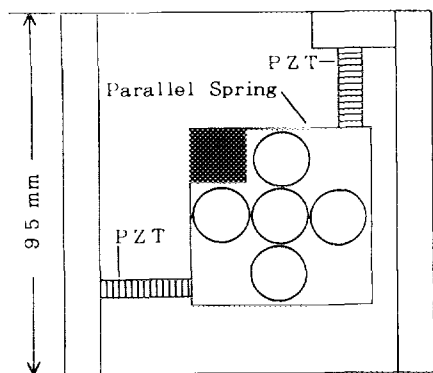


FIG. 3. Schematic diagram of the monolithic parallel spring.

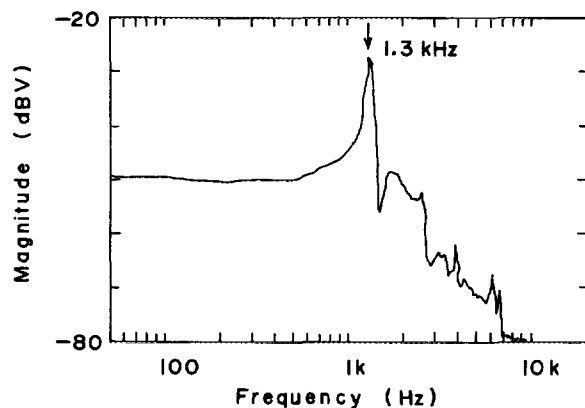


FIG. 4. Mechanical frequency response of the STM unit in the  $z$  direction.

Judging from above experimental results, our STM unit has a high stiffness, thereby acquiring stable operation under mechanical and sound disturbances.

The mechanical vibration isolation was achieved with the five stacked type,<sup>13,14</sup> which was constructed with brass plates and lead plates, and rubbers [vibration- and impact-absorber (Gelnac N-15C, Japan Automation Ltd.)], which have a very high impact absorption coefficient of about 97%. We put the STM system on an ordinary laboratory table.

**III. RESULTS AND DISCUSSION**

The STM images was observed in air at room temperature, and at the constant-current mode and the zero bias voltage. Mechanically fabricated Pt/Ir (10% Ir) tips were used in this work. The experimental results were observed with an oscilloscope and a XY recorder using a display controller constructed in our laboratory.

Figure 6 shows the STM image of a gold thin film evaporated on a glass plate observed on an oscilloscope. The scanning range in the  $x$  and  $y$  directions is  $1.1 \times 1.4 \mu\text{m}^2$ . The sample bias voltage is  $64 \text{ mV}$ , and the tunneling current is

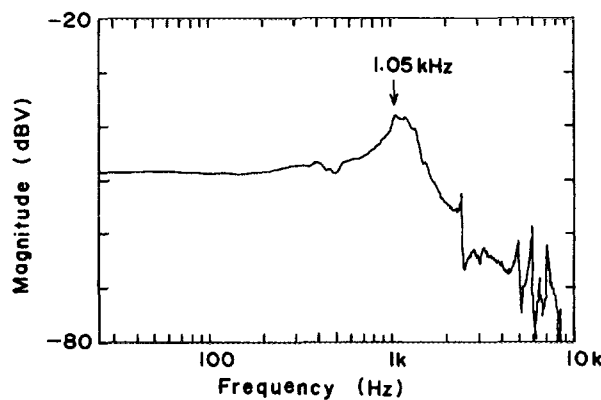


FIG. 5. Mechanical frequency response of the STM unit in the  $x$  direction.

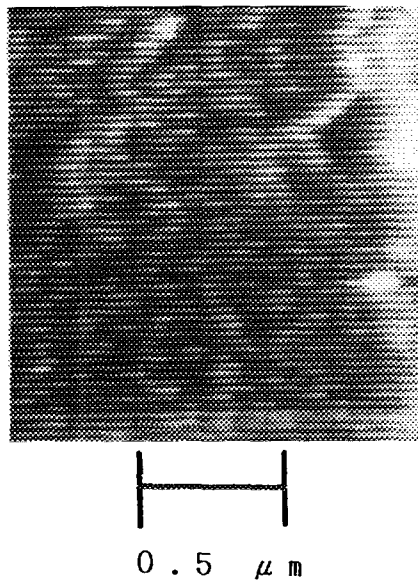


FIG. 6. STM image of gold thin film on a glass plate. The sample bias voltage is 64 mV, and the tunneling current is 0.4 nA.

0.4 nA. The film is formed with collecting gold clusters in diameter of about 100 nm, which is equivalent to other STM observation results.<sup>15-17</sup>

Figure 7 shows the STM images of a standard block

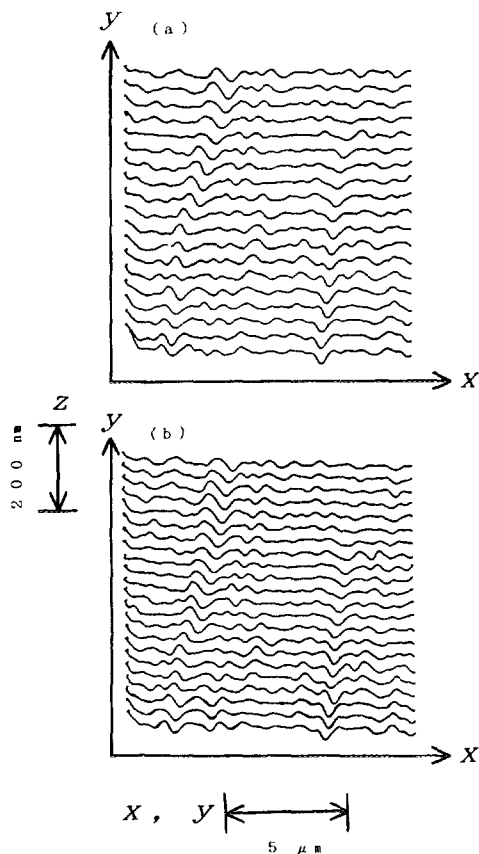


FIG. 7. STM images of a block gauge. The sample bias voltage is 64 mV, and the tunneling current is 0.66 nA. (a)  $y$ -direction scanning. (b)  $-y$ -direction scanning.

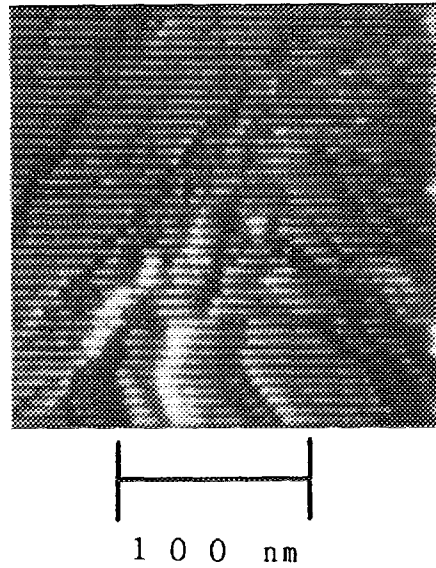


FIG. 8. STM image of a block gauge. The sample bias voltage is 64 mV, and the tunneling current is 0.46 nA.

gauge, which is used to calibrate industrial length or micrometers. The block gauge surface coated with rust preventing oil was cleaned with an acetone solvent. The scanning range in the  $x$  and  $y$  directions is  $12 \mu\text{m}$ . The sample bias voltage is 64 mV, and the tunneling current is 0.66 nA. In Fig. 7(a), a scanning direction is  $+y$ , and in Fig. 7(b) a scanning direction is  $-y$ . The STM images of Figs. 7(a) and 7(b) agree precisely; therefore, we consider that our STM is a stable and reproducible system. We find a regular rugosity with a  $R_{\text{max}}$  (maximum peak-to-valley height) value of 40 nm and with about  $0.7 \mu\text{m}$  roughness wavelength. The surface roughness has been measured with STM, and the roughness curves have been analyzed.<sup>3,18-21</sup> The relationship between  $R_{\text{max}}$  and measuring length  $L$  was given by  $R_{\text{max}} \propto L^D$ , where the value of  $D$  using a block gauge surface was calculated at 3,<sup>20</sup> and  $D$  using a finished gold surface at 0.6.<sup>21</sup> The value of  $D$  estimated using our experimental results is about 3. This value agrees well with a result calculated by Valdes, Lobbe, and Porfiri<sup>20</sup> using a roughness curve published by Garcia *et al.*<sup>3</sup> The cause of disagreements would be the difference of surface finishing methods and materials. The power spectrum of the roughness curve as shown in Fig. 7 has a  $1/f^3$  frequency dependence. This result agrees with other roughness curves observed with STM.<sup>20,21</sup> We cannot observe these small surface roughness with a standard stylus instrument.

Figure 8 shows the STM image of a block gauge. The scanning range is  $0.22 \mu\text{m}$ . The sample bias voltage is 64 mV, and the tunneling current is 0.46 nA. The observed corrugations and steps will be related to a superfinished surface and/or material properties. Figure 9 shows the STM image of a block gauge observed at the zero bias voltage and in the same position shown in Fig. 8. The control tunneling current is 0.26 nA. Our STM system can control with the tunneling current noise caused by the tunneling resistance. Therefore, the STM system constructed is a low electronic and mechanical noise. The STM image of Fig. 9 agrees with that

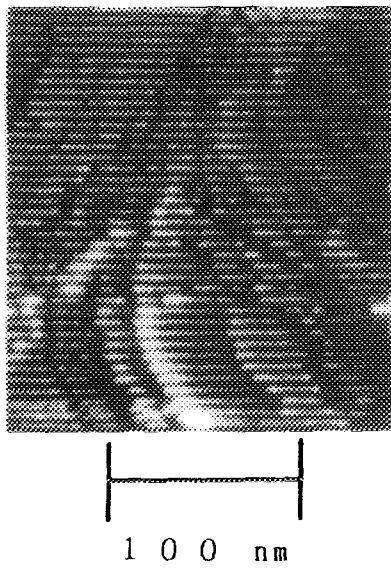


FIG. 9. STM image of a block gauge. The sample bias voltage is 0 V, and the control tunneling current is 0.26 nA.

of Fig. 8. Therefore the generation mechanism of surface corrugations, which is a function of surface topography and barrier height properties, will be similar in the both surface imaging method.

A block gauge is made from steel, which has in general metallic oxides over the sample with a very different resistivity.<sup>18</sup> The STM images and the zero bias voltage images observed are stable and reproducible. We consider the reason for this as follows: The block gauge surface may be covered with an oil thin film, and the STM tip may be scanned in this film; therefore, the effect of oxidation may be small. These observation methods will be important in the following field. The nanostructures on smooth or superfinished surfaces, which are required in the field of the precision engineering, the nanotechnology, and the optical and x-ray elements, can be evaluated using the STM operated in air.

#### IV. SUMMARY

A new scanning tunneling microscope and its application to surface roughness observation is described. Precision two-dimensional positioning of our STM instrument was achieved with a two-dimensional parallel spring driven by two stacked piezoelectric actuators (PZT). The PZT for the

z-axis displacement and control was mounted on the monolithic parallel spring. Therefore, the mutual interference effect of three-dimensional displacements is negligible. We have applied this STM to observation of surface roughness. A gold thin film evaporated on glass plates and a block gauge are observed at the constant-current mode and the zero bias voltage. The roughness curve is analyzed, and the results agree with previous experiments. These methods will be applied to the precision engineering, the nanotechnology, and the optical and x-ray elements.

#### ACKNOWLEDGMENTS

This work has been supported in part by Mitutoyo Ltd., the Manufacturing Technology Center of Shizuoka University, and a Grant-in-Aid from the Ministry of Education, Science and Culture of Japan.

- <sup>1</sup>G. Binnig, H. Rohrer, Ch. Gerber, and E. Weibel, *Phys. Rev. Lett.* **50**, 120 (1983).
- <sup>2</sup>S. Park and R. C. Barrett, in *Scanning Tunneling Microscopy*, edited by J. A. Stroscio and W. J. Kaiser (Academic, San Diego, 1993), p. 31.
- <sup>3</sup>N. García, A. M. Baró, R. Miranda, H. Rohrer, Ch. Gerber, R. García Cantú, and J. L. Peña, *Metrologia* **21**, 135 (1985).
- <sup>4</sup>B. Binnig and H. Rohrer, *Helvetica Acta* **55**, 726 (1982).
- <sup>5</sup>G. Binnig and D. P. E. Smith, *Rev. Sci. Instrum.* **57**, 1688 (1986).
- <sup>6</sup>F. E. Scire and E. C. Teague, *Rev. Sci. Instrum.* **49**, 1735 (1978).
- <sup>7</sup>H. Yamada, T. Fujii, and K. Nakayama, *Jpn. J. Appl. Phys.* **28**, 2402 (1989).
- <sup>8</sup>N. Tsuda, H. Yamada, M. Tanaka, K. Nakayama, F. Ishida, M. Hayashi, M. Miyashita, and M. Yamaguchi, *Proceedings of the International Conference on Advanced Mechatronics*, Vol. 451 (1989).
- <sup>9</sup>R. Moller, A. Esslinger, and B. Koslowski, *Appl. Phys. Lett.* **55**, 2360 (1989).
- <sup>10</sup>S. Grafstrom, J. Kowalski, and R. Neumann, *Meas. Sci. Technol.* **1**, 139 (1990).
- <sup>11</sup>S. Park and C. F. Quate, *Rev. Sci. Instrum.* **58**, 2010 (1987).
- <sup>12</sup>D. W. P. Pohl, *IBM J. Res. Dev.* **30**, 417 (1986).
- <sup>13</sup>M. Okano, K. Kajimura, S. Wakiyama, F. Sakai, W. Mizutani, and M. Ono, *J. Vac. Sci. Technol. A* **5**, 3313 (1987).
- <sup>14</sup>A. I. Oliva, V. Sosa, R. de Coss, R. Sosa, N. L. Salazar, and J. L. Pena, *Rev. Sci. Instrum.* **63**, 3326 (1992).
- <sup>15</sup>A. Sasaki, F. Iwata, A. Katsumata, J. Fukaya, H. Aoyama, T. Akiyama, Y. Nakano, and H. Fujiyasu, *Jpn. J. Appl. Phys.* (to be published).
- <sup>16</sup>A. Sasaki, F. Iwata, A. Katsumata, S. Wanami, J. Fukaya, and H. Aoyama, *J. Jpn. Soc. Precision Eng.* **59**, 987 (1993).
- <sup>17</sup>A. Sasaki, H. Kawakami, K. Yamauchi, A. Nozaki, F. Iwata, J. Fukaya, A. Kosaka, H. Aoyama, and T. Kubo, *J. Jpn. Soc. Precision Eng.* **59**, 95 (1993).
- <sup>18</sup>R. García Cantú and M. A. Huerta Garnica, *J. Vac. Sci. Technol. A* **8**, 354 (1990).
- <sup>19</sup>D. R. Denley, *J. Vac. Sci. Technol. A* **8**, 603 (1990).
- <sup>20</sup>J. Valdes, E. Lobbe, and M. Porfiri, *Surf. Sci.* **181**, 262 (1987).
- <sup>21</sup>T. Yokohata, K. Kato, and K. Ohmura, *J. Vac. Soc. Technol. A* **8**, 585 (1990).